Resveratrol Inhibits the Formation of Multiple-Layered β-Sheet Oligomers of the Human Islet Amyloid Polypeptide Segment 22–27

Ping Jiang, Weifeng Li, Joan-Emma Shea, and Yuguang Mu

Support Information

Validate the force field parameters of resveratrol

To validate the force field parameters of resveratrol, we calculated the solvation free energy, ΔG_{sol}, in both Gaussian 09 and GROMACS simulation package (1). By employing the PCM (polarizable continuum model) solvation model in Gaussian(2), we determined the value of ΔG_{sol} to be -20.56 kcal/mol at B3LYP/6-31G** level. We also calculated ΔG_{sol} using the thermodynamic integration (TI) method. One resveratrol molecule was inserted into a cubic box filled with 1356 SPC water molecules. Then the system was subjected to a series of NPT simulations by using an increasing coupling parameter, λ. 19 equally spaced values of λ were chosen (λ=0.05, 0.10, 0.15 … 0.95. The starting potential energy function of the system is the fully interacting resveratrol and solvent, and the end state is two completely decoupled systems: resveratrol in vacuum and pure solvent. Electrostatic and Lennard-Jones interactions were separately turned off, and a soft-core potential was used to scale Lennard-Jones interactions (3-4). We chose a set of similar run parameters and the production simulation at each λ lasted for 2ns as similar in other's published work(4). The determined value of ΔG_{sol} is -17.98 kcal/mol by TI method which is reasonably consistent with the estimate of -20.56 kcal/mol by Gaussian. Therefore, we conclude that our molecular model for resveratrol is reliable.

Resveratrol is not a hydrophilic compound whose logP is ~3. Here we only consider the ratio of resveratrol and protein and not the concentration (which is ~0.31M in our system). A high concentration of resveratrol molecules will cause self-aggregation as shown in Figure S5. So we think our main conclusion will not sensitively dependent on the number of resveratrol.

Details of REMD simulations

The simulation of peptides enables us to look at the early stages of peptide aggregation. In order to study the inhibition mechanism, 12 small inhibitor molecules of resveratrol were added to the peptide system. We chose a comparable concentration of resveratrol to most *in vitro* experiments and achieved an inhibitory effect in a computationally feasible timescale (5-7). The insertion of inhibitors into the peptide system was random and close contacts with peptides was avoided. Our initial trial study on the inhibition mechanism employed a simpler system, composed of 4 random peptide chains with 10 resveratrol molecules similar to our previous study(8). However the inhibition effects did not show up in such a small system contrary to the evidently enhanced effects of a single lipid molecule on the aggregation of the four peptide chains(8). The running hypothesis was thus generated: 1) the inhibition effects can only be demonstrated in a larger system; 2) the inhibitory action may work on the fibril nucleation process. To test the hypothesis a larger system (7 peptide chains) as described above was constructed, in the meantime to keep the system as small as possible to allow replica exchange molecular dynamics (REMD) simulations feasible. Initially putting 4 peptide strands in a parallel β sheet template with three monomers standing by permits us to study the nucleation process directly.

and temperatures are listed here: 315.0K, 318.5K, 322.2K, 325.8K, 329.5K, 333.2K, 337.0K, 340.7K, 344.6K, 348.4K, 352.3K, 356.2K, 360.2K, 364.2K, 368.3K, 372.3K, 376.5K, 380.6K, 384.8K, 389.0K, 393.3K, 397.6K, 402.0K, 406.4K, 410.8K, 415.3K, 419.8K, 424.4K, 429.0K, 433.6K, 438.3K, and 443.1K. Each set of replica exchange simulations (one for the peptide system, and one for the combined peptide/inhibitor system) lasted for 500ns. The mixture of peptides and inhibitors was solvated in SPC water (1845 water molecules in hIAPP system and 1681 in hIAPP/resveratrol system). All bonds involving hydrogen atoms were constrained in length according to LINCS protocol (9). Electrostatic interactions were treated with the Particle Mesh Ewald (PME) method with a cutoff of 9 Å, and a cutoff of 14 Å was used for the van der Waals interactions (10). The integration step was set as 0.002 ps and non-bonded pair list was updated every 5 integration steps. The solutes and solvents were separately coupled to the external heat bath with the relaxation time of 0.1 ps. Replica exchange was attempted every 1000 integration steps (2 ps). The structure snapshots were output every 1 ps, and an ensemble of 500,000 structures at any temperature was produced for the analysis. Except properties monitored in a time period, all other analyses only used the data from the last 300 ns.

Figure S1

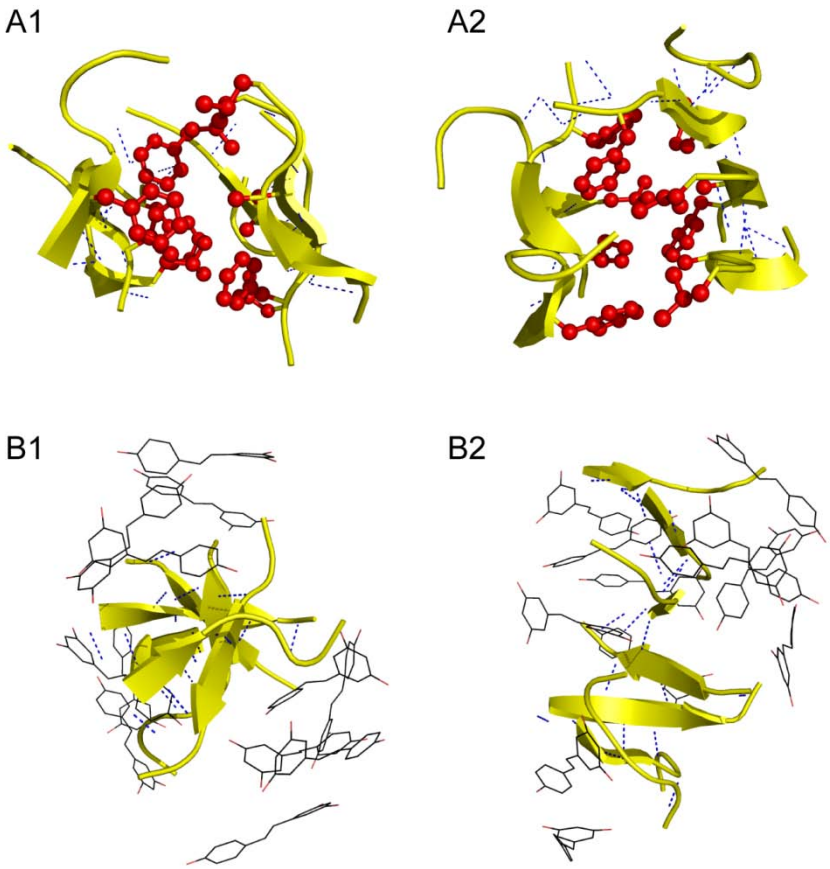

Figure S1. Representative structures of aggregates of size 7 in a β-barrel configuration in the absence of resveratrol (A1, A2) and in a single-layered configuration in the presence of resveratrol (B1, B2). Peptide backbones are shown in yellow, cartoon. In the absence of resveratrol (A1, A2), side chains wrapping inwards β-barrel are explicitly shown in red, ball-and-stick. In the presence of resveratrol (B1, B2), compounds surrounding peptides are shown. Dashed blue lines represent the hydrogen bonds formed on backbones.

Figure S2

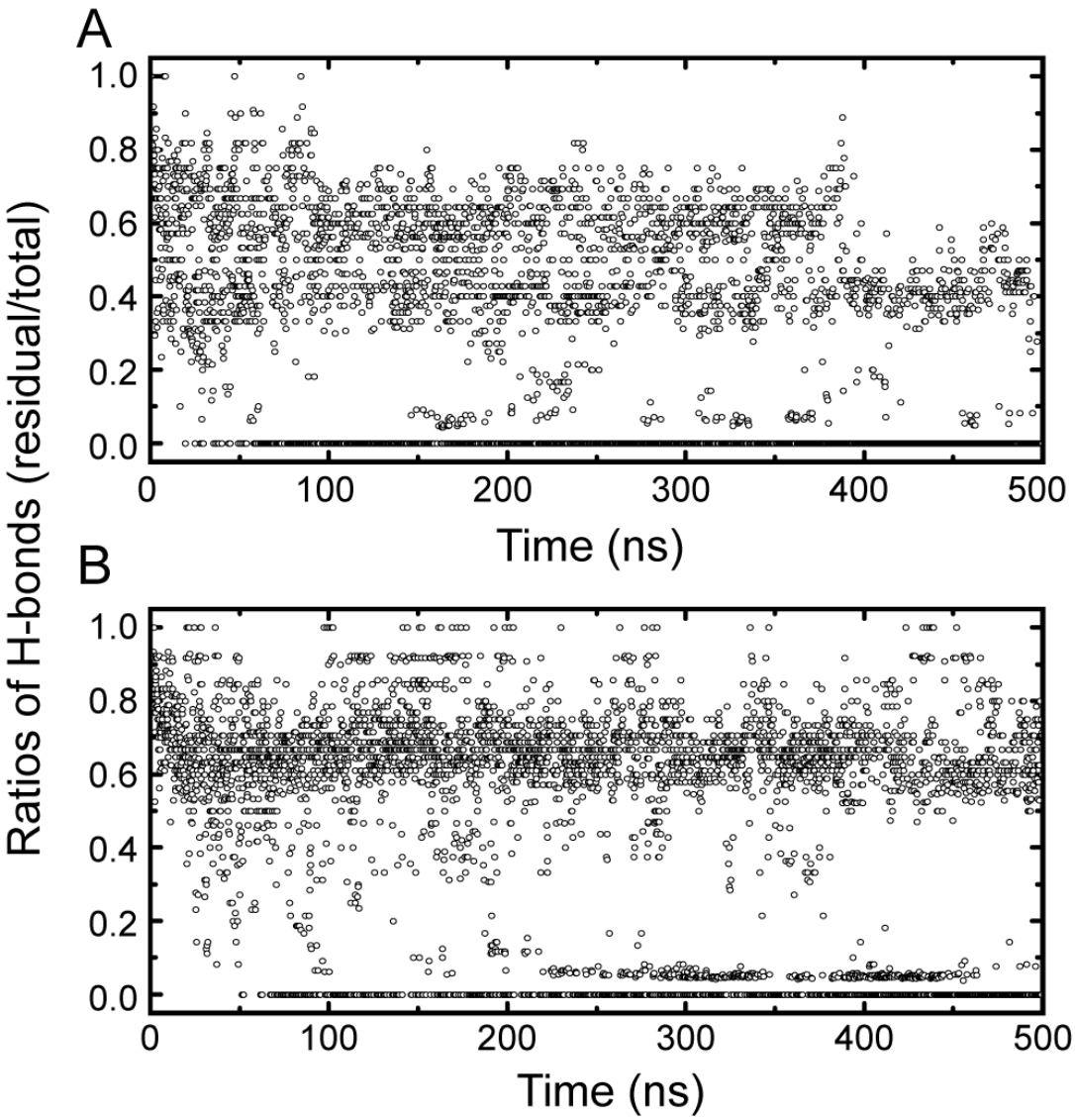

Figure S2. Tracing the residual hydrogen bonds preformed in the beginning of simulations. A ratio between the number of residual hydrogen bonds and that of the overall hydrogen bonds in each snapshot was calculated. (A) Time evolution of the ratio in the simulation of pure peptides. (B) Time evolution of the ratio in the simulation of peptides with resveratrol. For the sake of clarity, only a subset of all 500 ns data was shown here.

Figure S3

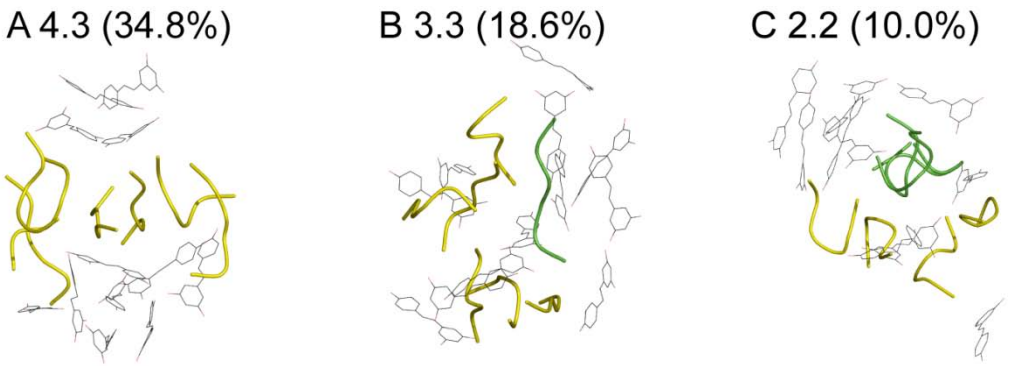

Figure S3. Representative structures of aggregates with double β-sheets in the presence of resveratrol - (A) tetramer-trimer, (B) double trimers, (C) double dimers. Peptides are shown in ribbons, yellow for oligomers and green for monomers. The resveratrol molecules are shown in black, line representation. The percentages in parentheses show the size of the first-ranked cluster in the overall aggregates with certain size.

Figure S4

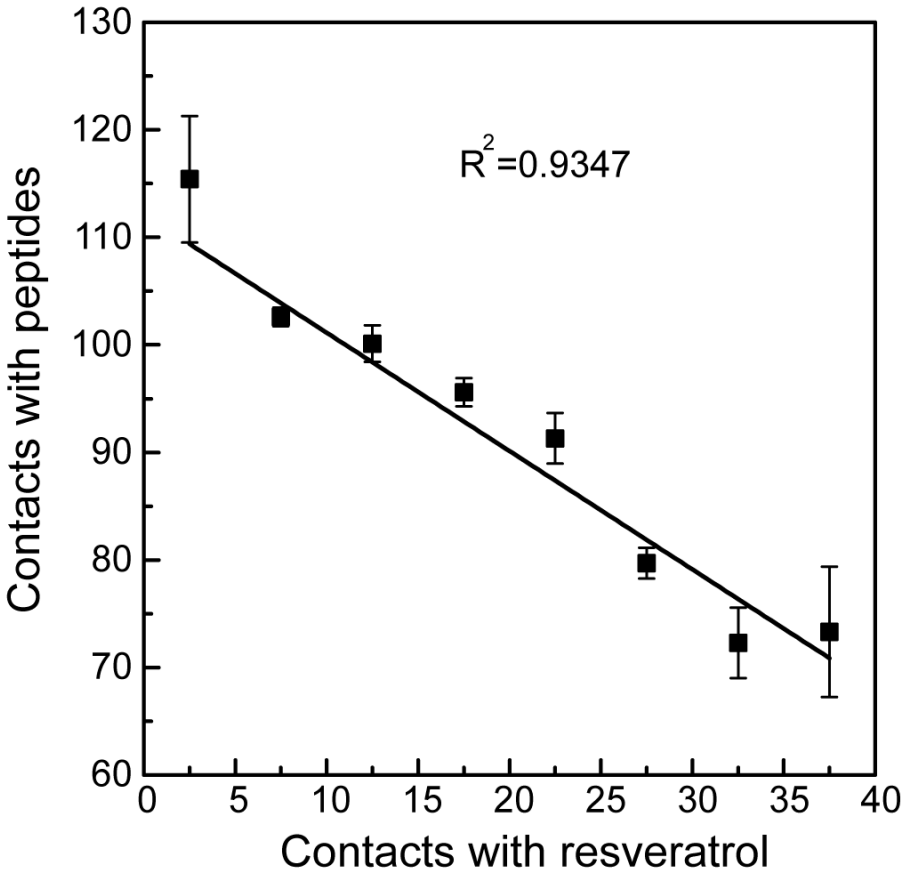

Figure S4. Correlation of side chain atomic contacts of the primary β-sheet with the rest peptides and with resveratrol molecules. Contact number with resveratrol (abscissa) was averaged over a bin of 5 contacts, and contact number with peptides (ordinate) was derived by averaging contacts of all data falling in the bin. Error bars indicate standard deviation of three time blocks: 200-300 ns, 300-400 ns, and 400-500 ns. The solid line is a linear fit to the data points. The two contacts are negatively linear-correlated.

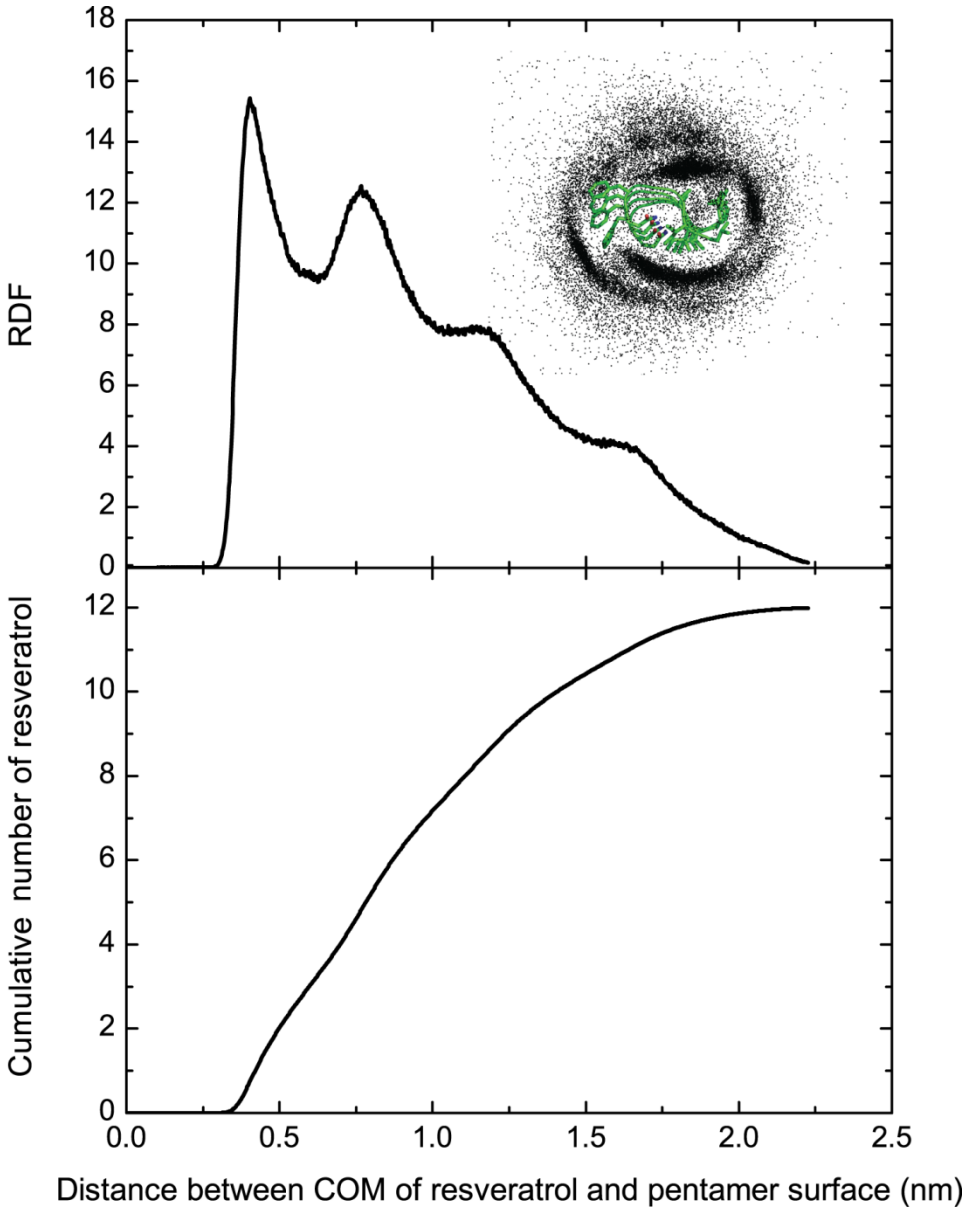

Figure S5. The radial distribution function (RDF) of resveratrol around pentamer (upper panel). The cumulative number of resveratrol around pentamer (lower panel).

RDF shows that there are roughly four stacking shells of resveratrol molecules around protein as shown in the inset figure. Based on the distance between the neighboring peaks (~0.4 nm), resveratrol molecules are face-to-face stacking. According to the cumulative number of small molecules, there are only three molecules within the fist shell, forming direct contacts with protein. Therefore, the effective ratio of protein and resveratrol is actually 5:3. The result agrees well with experimental result which suggested that the IC50 of resveratrol to IAPP should be 3.3:10(6).

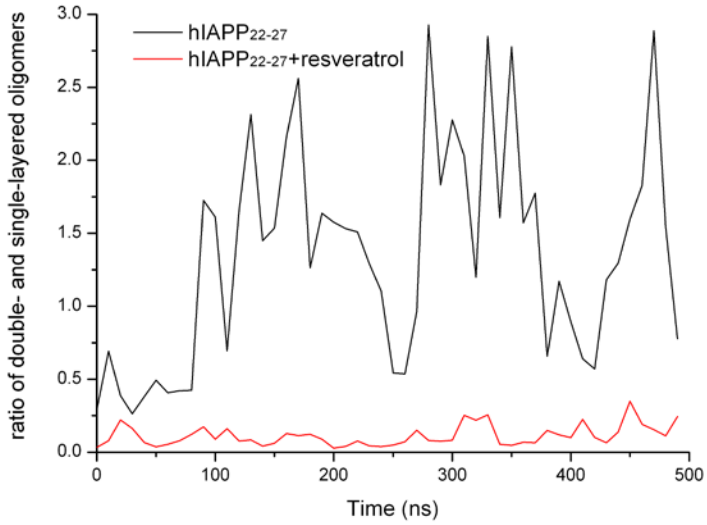

Figure S6
Evolution of ratio between double- and single-layered oligomers. After 100ns, although there is still big fluctuation, the order of magnitude is consistent. More importantly, the dominant oligomer species are clear and consistent for two systems.

1. David Van Der Spoel, E. L., Berk Hess, Gerrit Groenhof, Alan E. Mark Herman, J. C. Berendsen. 2005. GROMACS: Fast, flexible, and free. Journal of Computational Chemistry 26:1701-1718.
2. Scalmani, G., and M. J. Frisch. 2010. Continuous surface charge polarizable continuum models of solvation. I. General formalism. Journal of Chemical Physics 132:114110.
3. Steinbrecher, T., D. L. Mobley, and D. A. Case. 2007. Nonlinear scaling schemes for Lennard-Jones interactions in free energy calculations. J Chem Phys 127:214108.
4. Mobley, D. L., C. I. Bayly, M. D. Cooper, M. R. Shirts, and K. A. Dill. 2009. Small molecule hydration free energies in explicit solvent: An extensive test of fixed-charge atomistic simulations. J Chem Theory Comput 5:350-358.
5. Evers, F., C. Jeworrek, S. Tiemeyer, K. Weise, D. Sellin, M. Paulus, B. Struth, M. Tolan, and R. Winter. 2009. Elucidating the Mechanism of Lipid Membrane-Induced IAPP Fibrillogenesis and Its Inhibition by the Red Wine Compound Resveratrol: A Synchrotron X-ray Reflectivity Study. Journal of the American Chemical Society 131:9516-9521.
6. Mishra, R., D. Sellin, D. Radovan, A. Gohlke, and R. Winter. 2009. Inhibiting islet amyloid polypeptide fibril formation by the red wine compound resveratrol. Chembiochem 10:445-449.
7. Radovan, D., N. Opitz, and R. Winter. 2009. Fluorescence microscopy studies on islet amyloid polypeptide fibrillation at heterogeneous and cellular membrane interfaces and its inhibition by resveratrol. FEBS Lett 583:1439-1445.
8. Jiang, P., W. X. Xu, and Y. G. Mu. 2009. Amyloidogenesis Abolished by Proline Substitutions but Enhanced by Lipid Binding. Plos Computational Biology 5:e1000357.
9. Hess, B., H. Bekker, H. J. C. Berendsen, and J. Fraaije. 1997. LINCS: A linear constraint solver for molecular simulations. Journal of Computational Chemistry 18:1463-1472.
10. Darden, T., D. York, and L. Pedersen. 1993. Particle mesh Ewald: An N•log(N) method for Ewald sums in large systems. The Journal of Chemical Physics 98:10089-10092.